Prototypical solitons in the South China Sea

Jody M. Klymak,[1] Robert Pinkel,[1] Cho-Teng Liu,[2] Antony K. Liu,[3] and Laura David[4]

Received 10 February 2006; revised 14 April 2006; accepted 20 April 2006; published 9 June 2006.

[1] Surface signatures associated with non-linear internal waves are often seen in satellite images of the western South China Sea (SCS) slope and shelf. Observation in the deep sea, to the east, are rare. Here we report on the evolution of an energetic packet as it propagated through the deep central basin of the SCS, toward the western slope and shelf. The waves have amplitudes estimated at 170 m, half widths of 3 km, and phase speeds of 2.9 ± 0.1 m/s, faster than the mode-1 linear phase speed of 2.6 m/s. The shape and observed phase speed were consistent with the Korteweg-deVries (KdV) model over the 65-km path that they were tracked. The intrinsic velocity shear of the waves is small compared to pre-existing shears, and the waves exhibit weak turbulence. The KdV fit and a satellite-derived estimate of horizontal wave extent imply a westward energy flux of 4.5 GW for each crest. **Citation:** Klymak, J. M., R. Pinkel, C.-T. Liu, A. K. Liu, and L. David (2006), Prototypical solitons in the South China Sea, *Geophys. Res. Lett.*, *33*, L11607, doi:10.1029/2006GL025932.

1. Introduction

[2] Solitary waves in the South China Sea have been the subject of recent focused study [*Lynch et al.*, 2004]. The waves are internal, but can be observed via their surface expression in satellite imagery. They appear to originate near the Straits of Luzon and propagate westward across the basin until they encounter the Chinese shelf [*Zhao et al.*, 2004]. Considerable effort has gone into understanding the characteristics of these waves on the shelf, but little is known about them in the deep basin. Their origin, propagation speed, vertical structure, evolution, and energy flux remain to be documented by in situ observations.

[3] Solitary waves often form when a forced internal wave steepens and develops a nonlinear leading edge. The leading undulations are often compared to classical sech^2 solitary wave solutions of the Korteweg-deVries (KdV) equation, in which a weak nonlinear term balances the tendency of the wave shape to disperse. However, it is rarely observed that the waves maintain the KdV shape for long. In the Sulu Sea, *Apel et al.* [1985] tracked a series of waves from generation at an island chain to their dissipation on a shelf. The waves changed shape and amplitude, attributed to radial spreading and turbulence dissipation [*Liu et al.*, 1985]. Similar wave-tracking exercises on the Oregon Shelf of both waves of depression [*Moum et al.*, 2003] and waves of elevation [*Klymak and Moum*, 2003] demonstrate significant evolution of the waves over time and space (J. Moum, personal communication, 2006). Thus the term "solitary wave" has been deemed somewhat inaccurate, and the term "solibore" has been suggested [*Henyey and Hoering*, 1997].

[4] Solitary waves in shallow water are often very dissipative, and exhibit rapid spatial evolution. On the New England shelf, they play an important role in the energy budget, causing more dissipation than non-storm inertial waves [*MacKinnon and Gregg*, 2003]. Coastal solitary waves often exhibit strong shears and generate turbulence due to shear instability [*Moum et al.*, 2003]. Deep-sea solitary waves, in contrast, are associated with relatively little shear. They can, however, trigger mixing events on pre-existing background shears [*Pinkel*, 2000].

2. Experiment

[5] Observations were obtained from the *R/V Revelle*, 15 April–15 May, 2005 (Figure 1). Velocity data were collected with a 140 kHz Doppler sonar developed at Scripps Institution of Oceanography. The vertical resolution of the sonar is 6 m to approximately 200 m depth. One minute averages have an accuracy of 2 cm/s. The sonar also returns backscatter intensity, which is used to qualitatively visualize the waves.

[6] Salinity and temperature were sampled with a fast CTD profiler based on a Sea Bird Instruments SBE49. The profiler consisted of a streamlined body weighing 20 kg in air attached to a thin cable. This was cycled vertically at speeds exceeding 5 m/s, allowing drops to 500 m depth every 6 minutes.

3. A Representative Wave Packet

[7] We focus on a packet of deep-water waves that we followed westward from the Luzon Strait on 28 April 2005. The lead crest was first encountered at 119.6 E (Figure 2). The vertical excursion of parcels of water in this wave reach 100 m at the depths we observed. Backscatter intensity closely tracks isopycnals on the large-scale, and reveals further fine-scale detail. There are strong velocities concentrated near the surface in the wave (Figure 2b), with peak westward velocities of 2 m/s. The northward velocity (not shown) is small, and not coherent with the wave. The horizontal velocity signature decreases with depth, and is difficult to distinguish by 250 m.

[8] The shear field in this example is particularly rich (Figure 2c). The wave appears to be advecting pre-existing shear that has 50 m vertical wavelengths, possibly of near-inertial origin. The shear layer near $\sigma_\theta = 22.5$ appears susceptible to shear instability using the Richardson number

[1] Scripps Institution of Oceanography, La Jolla, California, USA.
[2] Institute of Oceanography, National Taiwan University, Taipei, Taiwan.
[3] Office of Naval Research Global–Asia, Tokyo, Japan.
[4] Marine Science Institute, University of Philippines, Manila, Philippines.

0094-8276/06/2006GL025932$05.00

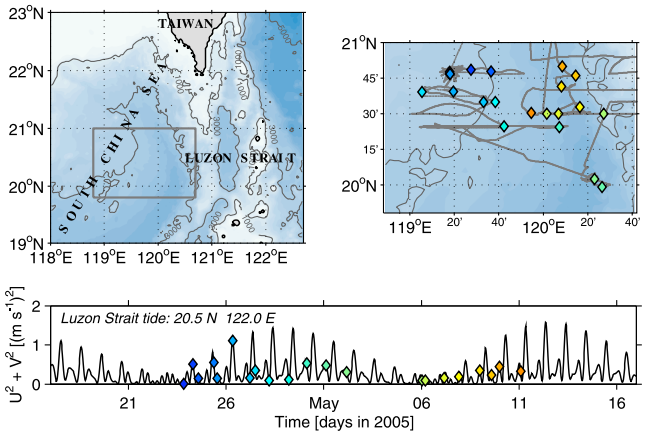

Figure 1. The study site was in the deep basin of the South China Sea, west of the Luzon Strait, April–May, 2005. Solitary wave events are indicated on the map on the right, color-coded by time. The same events are noted relative to the barotropic tide at 122 E 20.5 N, in the Luzon Strait, in the bottom panel. We did not sample the region May 3 to May 5.

criterion (Figure 2c). This layer is co-located with high-horizontal-wavenumber oscillations at the leading edge of the wave. The fastest-growing wavelength λ for a shear instability is $2\pi\lambda^{-1} h \approx 0.5$[*Hazel*, 1972]. Here, $h \approx 30$ m is the shear layer thickness, giving $\lambda \approx 377$ m. If we assume the oscillations are passively advected by the velocity they are embedded in, then we can use the ship's navigation and sonar-derived estimates of relative velocity to correct for the Doppler shift. The observed $\lambda \approx 350$ m. Therefore one candidate source for these oscillations is shear instability. The other possibility is that the oscillations are pre-existing and perhaps amplified by interaction with the solitary wave. In either case, we do not see similar feature in other waves observed that day. This suggests that they are intrinsic to the background shear field, not part of the solitary wave.

[9] To document the presence of turbulence in this wave we looked for overturns in the density profiles [*Alford and Pinkel*, 2000]. Large overturns are seen in two CTD profiles at the crest of the wave where the Richardson number is low. Estimated dissipation exceeds $\varepsilon \approx 10^{-5}$ m^2/s^{-3}. However, the turbulence lasts for only 10 minutes (or 600 m in the wave's frame). Other crests in the packet do not show significant turbulence, nor do subsequent observations of this crest. We conclude that this small-scale activity is also part of the background wavefield, perhaps enhanced by the passage of the solitary wave.

4. Wave Properties

[10] This wave was the first in a packet of waves that we tracked westward, passing through the packet five times during a 6-h period (Figure 3). A satellite image taken 3 h after we stopped indicates at least three waves. Averaged from the position of the first encounter to the satellite image, the phase speed of the lead wave is 2.97 m/s, and the second wave 2.92 m/s. The third wave in the packet has more curvature, but appears to have a similar phase speed. These phase speeds are faster than the linear, high-frequency, mode-1 phase speed of 2.6 m/s, calculated from a deep density profile. Topographic changes between 118.5 and 120 E are sufficient to change the linear phase speed by only 0.1 m/s, so in the absence of strong fronts, the waves are passing through a relatively homogeneous environment. Before the waves pass, a westward background current of $u \approx -0.1$ m s^{-1} is observed, which could advect the waves more quickly.

[11] Given the nearly constant phase speeds observed, it is useful to put the observation in a co-ordinate frame moving with the packet: $x_w = x - ct$. Here x is the geographic position, t is time (in seconds) and $c = 2.97$ m/s (Figure 4). In this frame, the waves have a roughly sech^2 shape with a half-width of 3 km. The front two crests are similar in shape, and 10 km apart. Eight hours later, the satellite image indicates that they are 10.9 km apart.

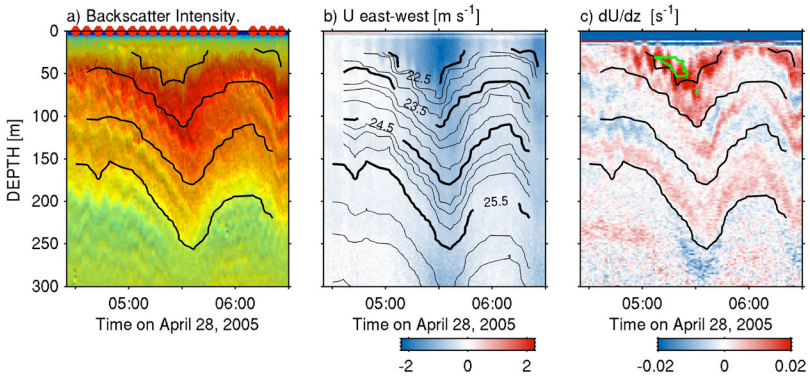

Figure 2. Solitary wave observed at 20.6 N, 119.63 E, 28 April 2005, 06:30 UTC. Contours are isopycnals (labeled in b). a) logarithm of acoustic backscatter intensity, scaled by the range as r^4 (no units). Diamonds indicate CTD casts. b) east-west velocity. The velocities are westward and north-south velocities are much smaller. c) East-west vertical shear. Green contour is where $Ri^{-1} > 4$; note that we do not have estimates of 10-m shear shallower than 25 m, so unstable shear could exist shallower than is pictured.

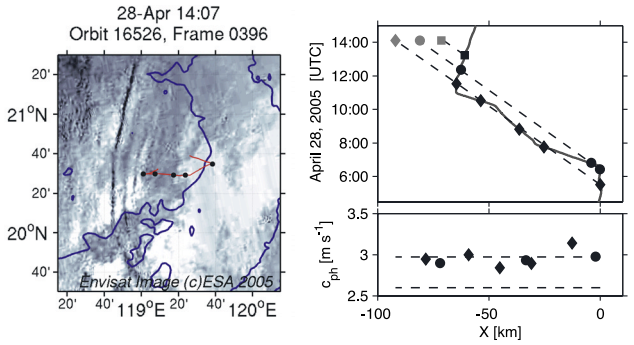

Figure 3. Wave tracking. Left panel is a satellite image taken 7.5 hours after the first encounter with the lead wave. Ship track is shown in red, and wave encounters are signified by black dots; the wave in Figure 2 is the easternmost encounter. The blue contour is the 3000-m isobath. Right panel is a time-space plot of the wave tracking. The lead wave (Figure 2) was encountered 5 times by the ship, and once by the satellite (diamonds). A second wave was seen three times by the ship and once in the satellite (circles), and a third wave once by the ship and satellite (squares). Phase speed from first-differencing the space and time are estimated for the waves in the lower right panel. The average phase speed of the lead wave is the upper dashed line, the linear phase speed is the lower.

[12] We fit the two lead waves to the KdV equation in a stratified fluid [*Ostrovsky and Stepanyants*, 1989]. We determine the structure of the first vertical displacement mode $\hat{w}_1(z)$ from the vertical stratification $N^2(z)$ [i.e., *Gill*, 1982]. The solution to the KdV equation is

$$\eta = \eta_o \mathrm{sech}^2\left(\frac{x - c_p t}{\Delta}\right), \tag{1}$$

where η_0 is the wave amplitude, the phase speed of the solitary wave is $c_p = c_1 + \alpha\eta_0/3$, and the width of the wave is given by $\Delta^2 = 12\beta/(\alpha\eta_0)$. α and β are functions of $\hat{w}_1(z)$ and c_1.

[13] The displacement of the water column due to the wave, $\eta(x, z)$, is calculated from the observed density field, and then normalized by the vertical mode shape to get a depth-averaged wave displacement:

$$\overline{\eta}(x) = (z_2 - z_1)^{-1} \int_{z_1}^{z_2} \eta(x,z) \frac{\hat{w}_1(885)}{\hat{w}_1(z)}\, \mathrm{d}z, \tag{2}$$

where 885 m is the depth where mode-1 has its maximum vertical displacement. This calculation is noisy near the surface where $\hat{w}_1 \approx 0$, and near the bottom of the domain where η is poorly defined, so we chose $z_1 = 350$ m and $z_2 = 55$ m. The results are the dots Figure 4c. A linear regression to fit $\overline{\eta}$ to a sech^2 shape yields an amplitude of $\eta_0 = 170$ m. We vary η_o by 20 m in a KdV solution to get an idea of how much the waveforms and the wave-fit characteristics vary (Table 1).

[14] The KdV phase speed is $c_{ph} = 2.9$ m/s, slower than the observed phase speed by 0.07 m/s. The small difference is consistent with the background currents, variations in bathymetry, and the imprecision of the KdV model. The same fit is used for the lead two crests in the packet after they have traveled 65 km. Over the six hours, the pair of waves do not appear to have significantly changed form. Their spacing increased by 900 m, indicating that the lead wave is slightly faster. We are not aware of observations that have found continuous agreement in both shape and phase speed over such a long observation length.

[15] Having a model allows us to estimate the energy in a soliton crest (Table 1). For the calculation we assume each crest is truly solitary, isolated from the others with the fit sech^2 waveform. Kinetic energy density is given by:

$$KE = \frac{1}{2} \int_{-H}^{0} \int_{-L}^{L} \rho\left(U^2 + W^2\right)\, \mathrm{d}x\, \mathrm{d}z, \tag{3}$$

where the theoretical model waveforms are used to extrapolate from the observed depth range to full ocean depth. This yields $KE = 1.1$ GJ/m.

[16] The available potential energy requires more care to calculate:

$$APE = \int_{-H}^{0} \int_{-L}^{L} g(\rho - \overline{\rho}) z \mathrm{d}x\, \mathrm{d}z, \tag{4}$$

where $\overline{\rho}$ is determined by sorting the density in the domain of interest to its lowest potential energy state and then take the mean in x [*Hebert*, 1988]. The calculation of APE is sensitive to the size of the domain over which equation (4) is calculated; we found that the calculation converged for $L > 10\Delta$, approximately 40 km; we find $APE = 0.74$ GJ/m. Therefore $KE \approx 1.4\ APE$, lower than the ratio calculated for deep-water solitary waves by *Pinkel* [2000] and waves of elevation by [*Klymak and Moum*, 2003]. The solitary waves here have four orders of magnitude more energy than the waves on the Oregon shelf, and one order of magnitude more than those observed on the equator.

[17] The total energy in each crest is 1.8 GJ/m. The satellite indicates that the two lead waves fronts extend north-south 220 km. If, as our observations indicate, the wave packets are created every 24 hours by the tide, the two lead crests represent a 24-h average rate of energy flux of a little over 9 GW. There is additional energy contained in the trailing waves and in the background internal tide that is not considered here.

5. Discussion

5.1. Energy Implications

[18] The two lead solitary waves each carry approximately 1.8 GJ/m of energy westward across the South China Sea. If

Table 1. Parameters Used to Fit the KdV Equations[a]

η_0, m	c_1, m/s	α, s^{-1}	β, m^3 s^{-1}	c_{ph}, m/s	Δ, m	KE, J/m^{-1}	PE, J/m^{-1}
170 ± 20	2.6	-5.9×10^{-3}	7.2×10^5	2.90 ± 0.04	$2.94 \pm 0.2 \times 10^3$	$1.1 \pm 0.3 \times 10^9$	$0.75 \pm 0.1 \times 10^9$

[a]Amplitude was varied by 20 m to assess the uncertainties.

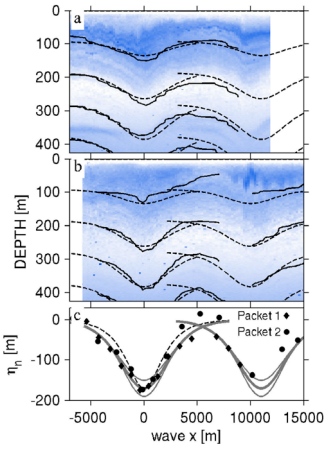

Figure 4. Lead two waves observed in first and last encounters. The x-co-ordinate is calculated relative to the lead wave crest, assuming the waves are moving to the west at 2.97 m/s. a) and b) Images are logarithm of backscatter intensity. Density from 100-m intervals are contoured in solid lines. Dashed lines are the same KdV fit applied to all four crests. c) Vertically averaged amplitude of the waves (symbols) compared to the fit (curves); see text for how the average is computed. Dashed line is the fit due to the nonlinear theory of *Joseph* [1977].

released daily, they comprise a 9 GW term in the local energy budget. These waves are among the largest we observed during the spring-neap cycle. If we assume the packet energy scales quadratically with barotropic velocity, then the fortnightly average will be 2.3 GW of energy. This can be compared to the energy flux of the internal semi-diurnal tide into the South China Sea, which is estimated from a numerical model to be 4.2 GW [*Niwa and Hibiya*, 2004], indicating that nonlinear waves are an important term in the energy budget.

[19] The observed waves are primarily diurnal, and modeling is just now being initiated to calculate the diurnal energy terms. Inverse modelling indicates that the diurnal component of energy may be larger than the semi-diurnal [*Egbert and Ray*, 2003]. Therefore, the solitary waves may be an important part of the energy budget, but we cannot yet quantify exactly how much energy the constitute.

5.2. Dissipation

[20] At one time in the propogation of this prototypical packet, the lead crest passed through shear strong enough to produce shear instabilities. The observed, small-scale wavelength was comparable to the most unstable mode of a classic Kelvin-Helmholtz instability. The instability is not consistent with the KdV solitary wave solution. The waves are mode-1, and their intrinsic shear is very low. Even the process of compressing upstream isopycnals posited by *Moum et al.* [2003] does not seem likely here. We believe that the strong, pre-existing shear layers (Figure 2c) are the most likely candidate, and that the high shear and short burst of turbulence in the lead wave is a coincidence, or at best slightly augmented by the solitary wave shear. The second wave, to which we fit the same amplitude KdV wave, was not observed to have a region of low Richardson number and did not have overturns.

[21] The solitary waves in the South China Sea appear to propagate without significant dissipation. They may trigger short bursts of dissipation when they pass through pre-existing shear from the inertial wave field, but this dissipation is not strong enough to change the amplitude or shape of the waves. The waves are "solitary" in the classic meaning of the term, in that they are form-invariant for over 60 km.

[22] **Acknowledgments.** The instruments used here were designed by the Ocean Physics Group, MPL/SIO/UCSD: E. Slater, M. Goldin, M. Bui, J. Pompa, T. Aja, and T. Hughen. Assistance at sea was provided by F. Delahoyd, T. Magno, T. Nan, and D. Wong. Thanks to the master and crew of the *R/V Roger Revelle*. Ren-Chieh Lien and Jonathan Nash provided insightful and constructive reviews. This work was supported by the Office of Naval Research, N00014-05-1-0140.

References

Alford, M. H., and R. Pinkel (2000), Observations of overturning in the thermocline: The context of ocean mixing, *J. Phys. Oceanogr.*, *30*, 805–832.

Apel, J. R., J. R. Holbrook, A. K. Liu, and J. J. Tsai (1985), The Sulu Sea internal soliton experiment, *J. Phys. Oceanogr.*, *15*, 1625–1651.

Egbert, G. D., and R. D. Ray (2003), Semi-diurnal and diurnal tidal dissipation from TOPEX/Poseidon altimetry, *Geophys. Res. Lett.*, *30*(17), 1907, doi:10.1029/2003GL017676.

Gill, A. E. (1982), *Atmosphere-Ocean Dynamics*, Elsevier, New York.

Hazel, P. (1972), Numerical studies of the stability of inviscid stratified shear flows, *J. Fluid Mech.*, *51*, 39–61.

Hebert, D. (1988), The available potential energy of an isolated feature, *J. Geophys. Res.*, *93*, 556–564.

Henyey, F. S., and A. Hoering (1997), Energetics of borelike internal waves, *J. Geophys. Res.*, *102*, 3323–3330.

Joseph, R. I. (1977), Solitary waves in a finite depth fluid, *J. Phys. A Math. Gen.*, *10*(12), L225–L227.

Klymak, J. M., and J. N. Moum (2003), Internal solitary waves of elevation advancing on a shoaling shelf, *Geophys. Res. Lett.*, *30*(20), 2045, doi:10.1029/2003GL017706.

Liu, A. K., J. R. Holbrook, and J. R. Apel (1985), Nonlinear internal wave evolution in the Sulu Sea, *J. Phys. Oceanogr.*, *15*, 1613–1624.

Lynch, J. F., S. R. Ramp, C.-S. Chiu, T. Y. Tang, Y.-J. Yang, and J. A. Simmen (2004), Research highlights from the Asian Seas International Acoustics Experiment in the South China Sea, *IEEE J. Oceanic Eng.*, *29*, 1067–1074.

MacKinnon, J., and M. Gregg (2003), Mixing on the late-summer New England shelf—Solibores, shear, and stratification, *J. Phys. Oceanogr.*, *33*, 1476–1492.

Moum, J. N., D. M. Farmer, W. D. Smyth, L. Armi, and S. Vagle (2003), Structure and generation of turbulence at interfaces strained by internal solitary waves propagating shoreward over the continental shelf, *J. Phys. Oceanogr.*, *33*, 2093–2112.

Niwa, Y., and T. Hibiya (2004), Three-dimensional numerical simulation of M2 internal tides in the East China Sea, *J. Geophys. Res.*, *109*, C04027, doi:10.1029/2003JC001923.

Ostrovsky, L. A., and Y. Stepanyants (1989), Do internal solitons exist in the ocean?, *Rev. Geophys.*, *27*, 293–310.

Pinkel, R. (2000), Internal solitary wave in the warm pool of the western equatorial Pacific, *J. Phys. Oceanogr.*, *30*, 2906–2926.

Zhao, Z., V. Klemas, Q. Zheng, and X.-H. Yan (2004), Remote sensing evidence for baroclinic tide origin of internal solitary waves in the northeastern South China Sea, *Geophys. Res. Lett.*, *31*, L06302, doi:10.1029/2003GL019077.

L. David, Marine Science Institute, University of Philippines, Velasquez Street, Manila 1101, Philippines.

J. M. Klymak and R. Pinkel, Scripps Institution of Oceanography, 9500 Gilman Dr., Box 0213 La Jolla, CA, 92093–0213, USA. (jklymak@ucsd.edu)

A. K. Liu, Office of Naval Research Global–Asia, 7-23-17 Roppongi, Tokyo 106-0032, Japan.

C.-T. Liu, Institute of Oceanography, National Taiwan University, P. O. Box 23-12 Taipei, Taiwan.